

## Crystal fields and magnetic interactions in $TmT_2Si_2$ (T = Co, Ni, Cu)

This article has been downloaded from IOPscience. Please scroll down to see the full text article.

2002 J. Phys.: Condens. Matter 14 2705

(<http://iopscience.iop.org/0953-8984/14/10/319>)

View [the table of contents for this issue](#), or go to the [journal homepage](#) for more

Download details:

IP Address: 171.66.16.27

The article was downloaded on 17/05/2010 at 06:18

Please note that [terms and conditions apply](#).

## Crystal fields and magnetic interactions in $\text{TmT}_2\text{Si}_2$ ( $\text{T} = \text{Co}, \text{Ni}, \text{Cu}$ )

S J Harker<sup>1,5</sup>, B D van Dijk<sup>1</sup>, A M Mulders<sup>2</sup>, P C M Gubbens<sup>1</sup>,  
G A Stewart<sup>3</sup>, C F de Vroege<sup>1</sup> and K H J Buschow<sup>4</sup>

<sup>1</sup> Interfacultair Reactor Instituut, Technische Universiteit Delft, 2629 JB Delft, The Netherlands

<sup>2</sup> Physics Department, Monash University, Clayton, Vic. 3168, Australia

<sup>3</sup> School of Physics, University College, The University of New South Wales, Australian Defence Force Academy, Canberra ACT 2600, Australia

<sup>4</sup> van der Waals–Zeeman Laboratory, University of Amsterdam, Valckenierstraat 65, 1018 XE Amsterdam, The Netherlands

E-mail: sjh@ph.adfa.edu.au

Received 25 October 2001

Published 18 March 2002

Online at [stacks.iop.org/JPhysCM/14/2705](http://stacks.iop.org/JPhysCM/14/2705)

### Abstract

An inelastic neutron scattering and  $^{166}\text{Er}$  Mössbauer spectroscopy study was performed on  $\text{ErCo}_2\text{Si}_2$  and a  $^{169}\text{Tm}$  Mössbauer spectroscopy study was performed on  $\text{TmT}_2\text{Si}_2$  ( $\text{T} = \text{Co}$  and  $\text{Ni}$ ). The saturation Er moment in  $\text{ErCo}_2\text{Si}_2$  was found to be  $7.8 \mu_{\text{B}}$  and the saturation Tm moment in  $\text{TmCo}_2\text{Si}_2$  was determined to be  $6.5 \mu_{\text{B}}$ . A crystal field interpretation of  $\text{ErCo}_2\text{Si}_2$  and  $\text{TmT}_2\text{Si}_2$  ( $\text{T} = \text{Co}$  and  $\text{Ni}$ ) is presented and, together with a new interpretation for existing data for  $\text{T} = \text{Cu}$ , trends in the crystal field parameters within the  $\text{TmT}_2\text{Si}_2$  series are presented.

### 1. Introduction

The  $\text{RT}_2\text{Si}_2$  ( $\text{R} = \text{rare earth}$ ,  $\text{T} = \text{transition metal}$ ) ternary compounds have long been of interest due to a range of novel magnetic properties [1–3]. The crystal field (CF) interaction in this series has been of interest as a source of information about s–f hybridization and has been investigated by changing the rare earth for  $\text{T} = \text{Cu}$  [4, 5]. Additionally a systematic investigation of the variation of the principal component,  $V_{zz}$ , of the electric field gradient (efg) tensor derived from the S-state ion  $\text{Gd}^{3+}$  for  $\text{GdT}_2\text{Si}_2$  [6–8] has shown an essentially linear variation across the transition metal series. However, the evolution of the CF parameters for  $\text{RNi}_2\text{Si}_2$  has been reported as not following the expected regular variation with rare earth [9]. A study of the effect on the CF of changing the transition metal for a fixed rare earth may improve the understanding of the local influences on the CF. For example, does the smooth

<sup>5</sup> Current address: School of Physics, University College, The University of New South Wales, Australian Defence Force Academy, Canberra ACT 2600, Australia.

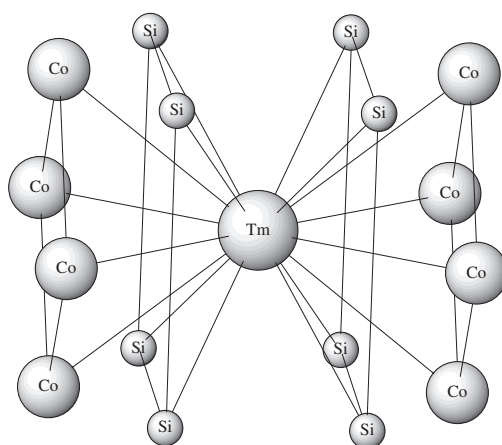


**Figure 1.** Thulium atom local site environment in  $\text{TmCo}_2\text{Si}_2$ , with the  $c$ -axis horizontal.

variation suggested by the Gd results persist for other rare earths? It is this question that is being investigated here. This work will consider the variation of CF parameters for heavy rare earth elements as T is varied from Fe through Co and Ni to Cu. Existing inelastic neutron scattering (INS) results for silicides with  $T = \text{Fe, Ni and Cu}$  are complemented by new INS data for  $\text{ErCo}_2\text{Si}_2$ .  $^{169}\text{Tm}$  Mössbauer data already exist for  $\text{TmFe}_2\text{Si}_2$  and  $\text{TmCu}_2\text{Si}_2$ , and new  $^{169}\text{Tm}$  Mössbauer data are presented here for  $\text{TmCo}_2\text{Si}_2$  and  $\text{TmNi}_2\text{Si}_2$ . The CF parameters determined from the INS data are tested against these  $^{169}\text{Tm}$  Mössbauer data.

The  $\text{RT}_2\text{Si}_2$  crystal structure is described by the prototype  $\text{ThCr}_2\text{Si}_2$ , having tetragonal space group  $I4/mmm$  ( $D_{4h}^{17}$ ). In this structure the single rare earth site's local symmetry (see figure 1) is tetragonal  $4/mmm$  ( $D_{4h}$ ). As long as higher-order electronic terms of a trivalent rare-earth ion can be ignored, the CF Hamiltonian for this symmetry may be written, in its simplest form, as

$$\mathcal{H}_{CF} = B_2^0 O_2^0 + B_4^0 O_4^0 + B_4^4 O_4^4 + B_6^0 O_6^0 + B_6^4 O_6^4, \quad (1)$$

where  $B_n^m = A_n^m \theta_n O_n^m(J)$  are CF parameters, and  $\theta_n$  are rare-earth specific factors associated with the Stevens operator equivalents,  $O_n^m$ , operating within the ground term having total angular momentum quantum number  $J$ . The parameters  $A_n^m$  are more convenient for comparison of the CF interaction across an isostructural series.

CF parameters have been reported in the literature for a wide range of  $\text{RCu}_2\text{Si}_2$  intermetallics, but for far fewer of the intermetallics involving other transition metals. Literature CF parameters for the rare earths are summarized in table 1 for the four transition metals (Fe, Co, Ni and Cu) considered here. It should be noted that for this symmetry the CF Hamiltonian is the same if *both*  $A_4^4$  and  $A_6^4$  change sign (corresponding to a coordinate frame rotation of  $45^\circ$  about the  $c$ -axis).

The  $\text{Gd}^{3+}$  ion is an S-state ion, so its 4f shell is not distorted by the CF interaction. Hence, for an ideal ionic lattice, the  $V_{zz}$  acting at its nucleus would derive entirely from the surrounding lattice and be related directly to the rank 2 CF parameter,  $A_2^0$ . For this reason, the most recent  $V_{zz}$  values measured for  $R = \text{Gd}$  using  $^{155}\text{Gd}$  Mössbauer spectroscopy [7, 8] are included in table 1. These values are in close agreement with the earlier  $V_{zz}$  values due to Nowik *et al* [6]. Also included in table 1 are the corresponding  $A_2^0$  values for  $R = \text{Tm}$  as converted from the  $V_{zz}$ . The  $A_2^0$  values obtained in this way suggest a linear progression across the transition metal series,  $T = \text{Fe, Co, Ni and Cu}$ , as revealed by the open circle data of figure 7. The  $A_2^0$

**Table 1.** Crystal field parameters for  $\text{RT}_2\text{Si}_2$  with rare earths, R, and transition metals, T = Fe, Co, Ni and Cu, as shown. In all cases the techniques employed are either Mössbauer effect spectroscopy (ME) or INS.

	$A_2^0$ (K)	$A_4^0$ (K)	$A_4^4$ (K)	$A_6^0$ (K)	$A_6^4$ (K)
<b>RFe<sub>2</sub>Si<sub>2</sub></b>					
Gd ME [7, 8]	+290.8	$(V_{zz} = -9.4(5) \times 10^{21} \text{ V m}^{-2})$			
Tm ME [10]	+251	-104	-300	0	-357
<b>RCo<sub>2</sub>Si<sub>2</sub></b>					
Gd ME [7, 8]	+160.8	$(V_{zz} = -5.2(2) \times 10^{21} \text{ V m}^{-2})$			
Er INS, this work	+181	-8.57	-151	+2.36	+84.0
Tm ME, this work	+232.7	-32.5	-572	+0.20	+7.12
<b>RNi<sub>2</sub>Si<sub>2</sub></b>					
Pr INS [11]	+171.8	+37.7	+318.5	+64.8	-90.7
Gd ME [7, 8]	+37.1	$(V_{zz} = -1.2(2) \times 10^{21} \text{ V m}^{-2})$			
Tb INS [12] 'A'	+95.3	+4.6	-94.8	+71	-836
Tb INS [12] 'B'	+97.7	+23.7	+464	+63.3	-942
Dy INS [9]	+45.2	-23.3	+48.6	+11.7	+179
Tm ME, this work	+137.9	+17.1	-35.7	-0.14	-2.13
<b>RCu<sub>2</sub>Si<sub>2</sub></b>					
Pr INS [4]	+34.8	-23.4	$\pm 353.8$	+10.0	$\pm 72.3$
Nd INS [4]	+56.0	-43.9	$\pm 53.0$	+9.7	$\pm 202.2$
Gd ME [7, 8]	-89.7	$(V_{zz} = +2.9(2) \times 10^{21} \text{ V m}^{-2})$			
Ho INS [4]	-146.2	-30.0	$\pm 46.4$	+4.04	$\pm 145.3$
Er INS, ME [13]	-65.4	-30.4	+80.4	+3.25	+156.0
Er INS [4]	-73.1	-33.2	$\pm 78.4$	+2.80	$\pm 162$
Tm ME [14]	+11.9	-191	-300	+24.3	-225
Tm ME, this work	-97.0	-24.5	+57.2	+3.6	+208
Yb INS [15]	-76.8	+140.7	$\mp 308.3$	-0.8	$\pm 133.3$

value reported for the earlier  $^{169}\text{Tm}$  investigation of  $\text{TmFe}_2\text{Si}_2$  is consistent with this trend, but there is a considerable discrepancy between the CF parameters reported for  $\text{TmCu}_2\text{Si}_2$  [14] and those obtained using INS for  $\text{ErCu}_2\text{Si}_2$  [4].

## 2. Experimental details and results

$\text{ErCo}_2\text{Si}_2$ ,  $\text{TmCo}_2\text{Si}_2$  and  $\text{TmNi}_2\text{Si}_2$  samples were prepared in an argon arc furnace and vacuum annealed for five weeks at 800 °C. The samples were characterized by x-ray powder diffraction and were found to be essentially single phase.

INS measurements were carried out on  $\text{ErCo}_2\text{Si}_2$  in the RKS 2 instrument at the Interfacultair Reactor Instituut at Delft. Spectra were taken at 9.5 and 12 K with neutrons of wavelength  $\lambda = 0.135 \text{ nm}$  and at 20 K with neutrons of  $\lambda = 0.2033 \text{ nm}$ . The 9.5 K INS spectrum is shown in figure 2.

$^{169}\text{Tm}$  Mössbauer spectra were recorded using absorbers of approximately  $9 \text{ mg cm}^{-2}$  of sample powder cooled (or heated) in a transmission geometry cryostat over the temperature range of 1.7–500 K. The source was a neutron-activated foil of  $^{168}\text{ErAl}_9$  mounted externally on a transducer and moved with sinusoidal motion. In Canberra the drive velocity was calibrated against a standard  $\text{TmF}_3$  absorber at 4.2 K, while in Delft the absolute velocity was calibrated with a laser Michelson interferometer.  $^{166}\text{Er}$  Mössbauer spectra were also recorded in Delft using a neutron-activated  $\text{HoPd}_3$  source and calibrated against a standard  $\text{ErFe}_2$  absorber at 4.2 K.

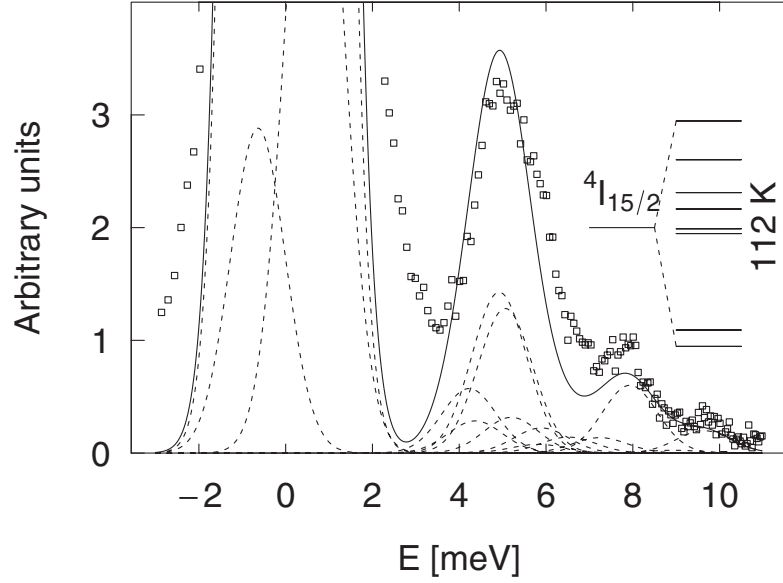


**Figure 2.** Neutron inelastic scattering from  $\text{ErCo}_2\text{Si}_2$  at an average scattering angle of  $37.3^\circ$  and a temperature of 9.5 K. The solid curve is the profile of the CF model, with the dashed curves being the separate CF transitions. The CF level diagram shown corresponds to the fit.

Representative  $^{169}\text{Tm}$  Mössbauer spectra for the paramagnetic phases of  $\text{TmNi}_2\text{Si}_2$  and  $\text{TmCo}_2\text{Si}_2$ , together with fits, are shown in figure 3. All paramagnetic phase spectra shown for both compounds could be analysed in terms of a single quadrupole-split doublet. The temperature-dependent quadrupole splittings,  $\Delta E_Q$ , are presented in figure 5, where they are compared with the earlier data for  $\text{TmFe}_2\text{Si}_2$  [10] and  $\text{TmCu}_2\text{Si}_2$  [14].

$\text{TmNi}_2\text{Si}_2$  is reported to order at  $T_{\text{order}} = 2.7$  K and to have  $\mu_{\text{sat}}(\text{Tm}) = 5.6 \mu_B$  [16], but no magnetically split patterns were observed down to our lowest temperature of 1.9 K. However, magnetically split Mössbauer spectra ( $^{169}\text{Tm}$  and  $^{169}\text{Er}$  respectively) were obtained for both  $\text{TmCo}_2\text{Si}_2$  and  $\text{ErCo}_2\text{Si}_2$ . The lowest-temperature spectra recorded are shown in figure 4. The fit to the 2.64 K magnetically ordered spectrum for  $\text{TmCo}_2\text{Si}_2$  yields a hyperfine field  $B_{\text{eff}} = 633.6$  T. This converts to  $\mu(\text{sat}) = 6.5 \mu_B$  if we assume that the ‘free ion’  $\text{Tm}^{3+}$  moment of  $7 \mu_B$  corresponds typically to a hyperfine field of 720 T in intermetallics [17] and is in good agreement with the  $\mu_{\text{sat}} = 6.2 \mu_B$  reported elsewhere [18]. For  $\text{ErCo}_2\text{Si}_2$  magnetic order sets in below  $\approx 9$  K. The fit to the 1.1 K  $^{169}\text{Er}$  spectrum yields  $B_{\text{eff}} = 676$  T, which converts to  $\mu(\text{sat}) = 7.8 \mu_B$ , taking the ‘free-ion’  $\text{Er}^{3+}$  moment of  $9 \mu_B$  as corresponding to 785 T [17]. This value is intermediate between the literature values of  $6.75 \mu_B$  at 4.2 K [19] with  $T_N = 6$  K and  $8.7(2) \mu_B$  at 4.2 K with  $T_N = 11$  K [20].

### 3. Crystal field interpretation

The INS spectrum for  $\text{ErCo}_2\text{Si}_2$  at 9.5 K (figure 2) shows three excitations at  $\Delta_1 \approx 5$  meV,  $\Delta_2 \approx 8$  meV and  $\Delta_3 \approx 9.5$  meV, which were identified as being due to the CF by the temperature independence of the  $Q$  value. The neutron scattering cross-section for transitions between the CF split levels was calculated by the standard formula [21]

$$\frac{d^2\sigma}{d\Omega_f d\omega_f} = N \left( \frac{1.91e^2}{2mc^2} g_J \right)^2 f^2(Q) \frac{k_f}{k_i} \sum \rho_n | \langle n | J_\perp | m \rangle |^2 \delta \left( \frac{E_n - E_m}{\hbar} - \omega \right), \quad (2)$$

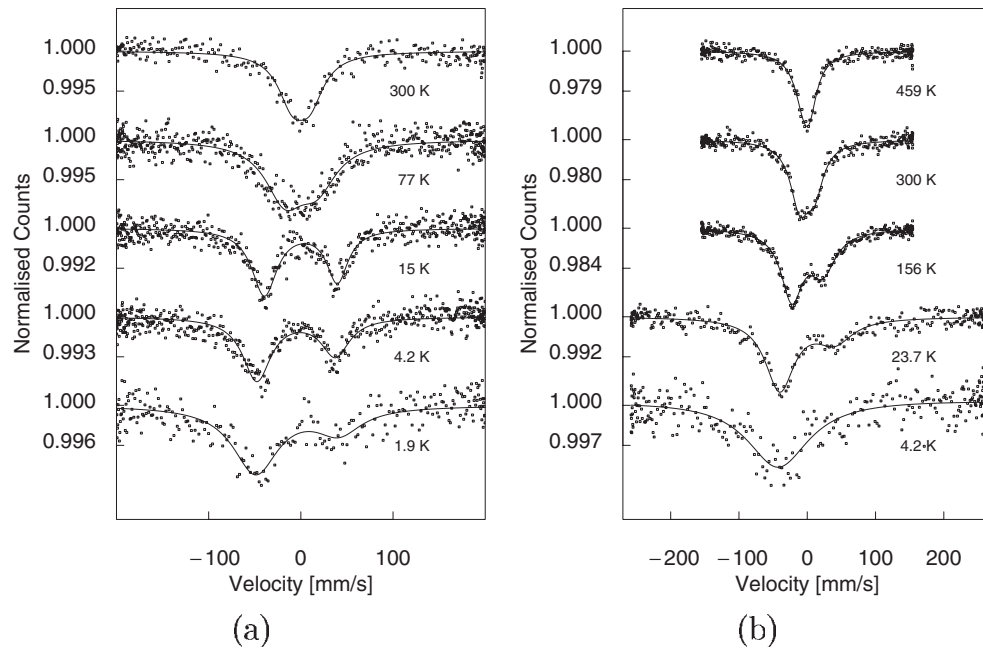


**Figure 3.** Representative paramagnetic  $^{169}\text{Tm}$  Mössbauer spectra for (a)  $\text{TmNi}_2\text{Si}_2$  and (b)  $\text{TmCo}_2\text{Si}_2$  at temperatures as shown. The full curves represent fits to the data.

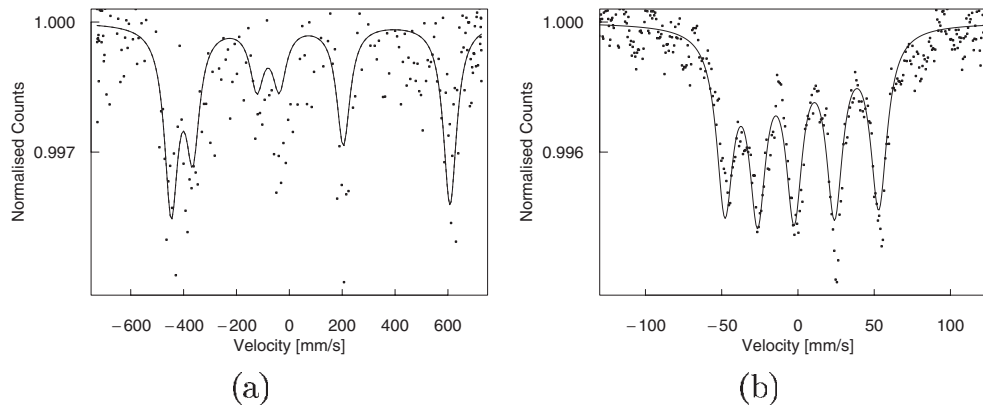


**Figure 4.** Magnetically ordered Mössbauer spectra of (a)  $\text{TmCo}_2\text{Si}_2$  at 2.64 K ( $^{169}\text{Tm}$ ) and (b)  $\text{ErCo}_2\text{Si}_2$  at 1.1 K ( $^{166}\text{Er}$ ); the full curves describe fits to the data.

where  $|n\rangle$  and  $|m\rangle$  are states belonging to a given  $J$  multiplet,  $J_{\perp}$  is the component of  $J$  perpendicular to the scattering vector  $Q$  and the other symbols have their usual meaning. Since equation (2) involves both the energies and intensities of the discrete number of possible transitions between CF levels it is, in principle, possible to find a unique solution for the set of five CF parameters. However, due to the overlap of transition peaks into three broad excitation features (figure 2), some ambiguity is introduced. This is one reason why a check of the CF analysis against data from other techniques is valuable. Here the initial fits were obtained with some constraints based on CF parameter sets published elsewhere for neighbouring

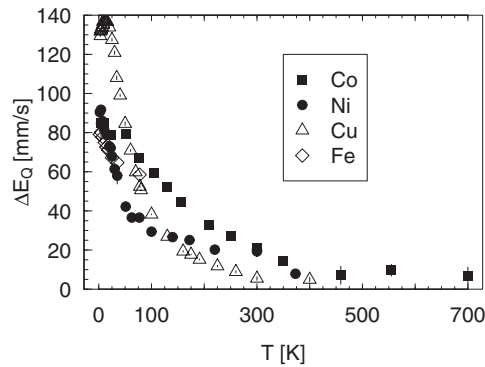


**Figure 5.** Comparison of experimental temperature-dependent  $\Delta E_Q$  values obtained for  $\text{TmT}_2\text{Si}_2$  for  $T = \text{Fe}$  [10],  $\text{Co}$  (this work),  $\text{Ni}$  (this work) and  $\text{Cu}$  [14].

intermetallics, while final fits were obtained with all CF parameters free to vary. Multiple solutions were obtained and the preferred set of CF parameters was selected on the basis of goodness of fit and by comparison with results for related compounds. The preferred set of CF parameters is given in table 1 and the fit to the INS spectrum is shown in figure 2, together with the corresponding CF level scheme which is comprised of eight Kramers doublets. The fitted value of  $A_2^0 = 181$  K is in good agreement with the value of 160.8 K converted from the  $^{155}\text{Gd}$  Mössbauer spectroscopy results for  $\text{GdCo}_2\text{Si}_2$ .

The quadrupole splitting,  $\Delta E_Q$ , determined from a  $^{169}\text{Tm}$  Mössbauer spectrum is a measure of the strength of the electric quadrupole interaction. For tetragonal site symmetry it is given by

$$\Delta E_Q = \left| \frac{1}{2} e Q V_{zz} \right| \quad (3)$$

where  $Q$  is the nuclear quadrupole moment of the 8.4 keV,  $I = 3/2$  nuclear level. The quadrupole splitting is a consequence of the direct lattice efg acting at the  $^{169}\text{Tm}$  nucleus plus the indirect temperature-dependent efg due to the CF distortion of the 4f shell. The theory is described elsewhere [22–24]. Given the link between quadrupole splitting and CF, the comparison of the experimental  $\Delta E_Q$  in figure 5 clearly demonstrates the sensitivity of the CF at the Tm site to the change in transition element.

Rather than attempting to fit all five CF parameters to the experimental  $^{169}\text{Tm}$  data, it was decided to fix the within-ranks ratios  $r_4^4 = A_4^4/A_4^0$  and  $r_6^4 = A_6^4/A_6^0$  to values based on existing INS-determined CF parameter sets given in table 1. This reduced the number of free parameters to just three:  $A_2^0$ ,  $A_4^0$  and  $A_6^0$ . Guided by a reasonable consistency for  $A_2^0$ , these ratios were based on CF parameters for the heavy rare earths located closest to Tm in the lanthanide series. The next problem was how to deal with the temperature-independent, lattice contribution to  $V_{zz}$ . For an ideal ionic lattice, this contribution can be related directly to the fitted  $A_2^0$ , as was assumed above when the  $^{155}\text{Gd}$   $V_{zz}$  results in table 1 were converted to  $A_2^0$ . However, Coehoorn *et al* [8] have used band structure calculations to demonstrate that, in Gd intermetallics, the two parameters have different origins. In particular there is a dominant 6p shell contribution to  $V_{zz}$ . The CF analysis of the  $^{169}\text{Tm}$  data was thus approached here using a fixed, independent lattice contribution to  $V_{zz}$ .

In summary, the approach adopted for testing the INS-determined CF parameters against the  $^{169}\text{Tm}$   $\Delta E_Q$  data was as follows.

- (i) Commence with a fixed lattice contribution to  $V_{zz}$  that is equal to the  $^{155}\text{Gd}$  value determined for isostructural  $\text{GdT}_2\text{Si}_2$ . If necessary vary the magnitude, but not the sign.

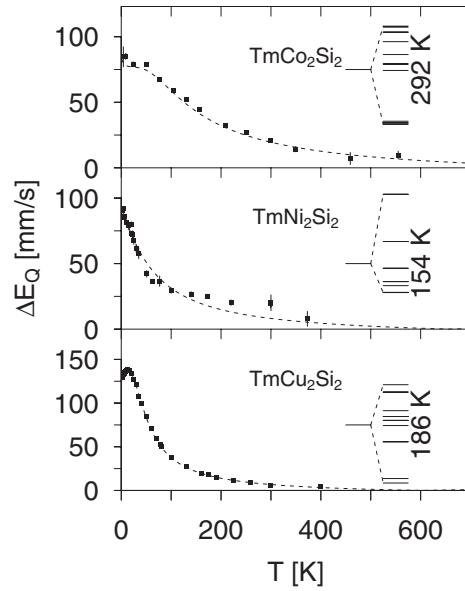


**Figure 6.** CF fits to the temperature dependence of  $\Delta E_Q$  obtained from  $^{169}\text{Tm}$  Mössbauer spectra of  $\text{TmT}_2\text{Si}_2$  ( $T = \text{Co, Ni and Cu}$ ) together with the appropriate CF level diagrams.

- (ii) Set the within-rank CF ratios to those determined using INS for the  $\text{RT}_2\text{Si}_2$  with R closest to Tm in the lanthanide series.
- (iii) Perform a least-squares grid search over  $A_2^0$ ,  $A_4^0$  and  $A_6^0$  with the sign of  $A_2^0$  restricted to that of the INS results for  $\text{RT}_2\text{Si}_2$ .

This approach was applied first to the earlier  $^{169}\text{Tm}$  data for  $\text{TmCu}_2\text{Si}_2$ , with  $r_4^4 = -2.36$ ,  $r_6^4 = 57.9$  (derived from the INS data for  $\text{ErCu}_2\text{Si}_2$  [4]) and  $V_{zz}^{\text{latt}} = +3 \times 10^{21} \text{ V m}^{-2}$  (from the  $^{155}\text{Gd}$  result for  $\text{GdCu}_2\text{Si}_2$ ). The best fit was achieved with  $A_2^0 = -94 \text{ K}$ ,  $A_4^0 = -39.2 \text{ K}$  and  $A_6^0 = -3.9 \text{ K}$ . An alternative, slightly poorer fit was achieved with  $A_2^0 = -97 \text{ K}$ ,  $A_4^0 = -24.5 \text{ K}$  and a positive  $A_6^0 = +3.6 \text{ K}$ . The second set of CF parameters is in very good agreement with the INS values for  $\text{ErCu}_2\text{Si}_2$  [4] and provides a much more consistent interpretation than the earlier CF parameters reported by Stewart and Zukrowski [14]. It is this set that is included in table 1 and the corresponding fitted theory curve is shown in figure 6.

The  $^{169}\text{Tm}$  data for  $\text{ErCo}_2\text{Si}_2$  were considered next. The INS results for  $\text{ErCo}_2\text{Si}_2$  (this work) give  $r_4^4 = +17.6$  and  $r_6^4 = +35.6$ . Because the  $^{169}\text{Tm}$   $\Delta E_Q$  data appear to plateau out at 400 K, a smaller lattice contribution of  $V_{zz}^{\text{latt}} = -3.3 \times 10^{21} \text{ V m}^{-2}$  was adopted, rather than the  $^{155}\text{Gd}$  result of  $-5.2 \times 10^{21} \text{ V m}^{-2}$ . The grid search resulted in a good description of the  $\Delta E_Q$  data as shown in figure 6. The  $A_2^0$  and  $A_6^0$  CF parameters (table 1) are also in reasonable agreement with the INS values for  $\text{ErCo}_2\text{Si}_2$ . However, the fitted  $A_4^0$  parameter is seen to compare less favourably than was the case for  $\text{TmCu}_2\text{Si}_2$ . Moreover, the fitted theory curve plateaus at a temperature much higher than the assumed 400 K.

As anticipated, the theory curve fitted to the  $^{169}\text{Tm}$  data for  $\text{TmNi}_2\text{Si}_2$  (using  $r_4^4 = -2.085$ ,  $r_6^4 = +15.3$  [9] and  $V_{zz}^{\text{latt}} = -2.8 \times 10^{21} \text{ V m}^{-2}$ ) provides only an approximate description, primarily because of the ‘step’ in the data around 300 K. The origin of this step is uncertain. A structural phase transition could explain it, but such a transition is not reported in the literature. It should be noted that the fit is reasonable for  $T \leq 50 \text{ K}$ . An additional complication is that  $^{169}\text{Tm}$  Mössbauer spectra of nickel-containing compounds suffer from poorer statistics due to the high absorption of the 8.4 keV gammas. This combines with the small  $\Delta E_Q$  values to



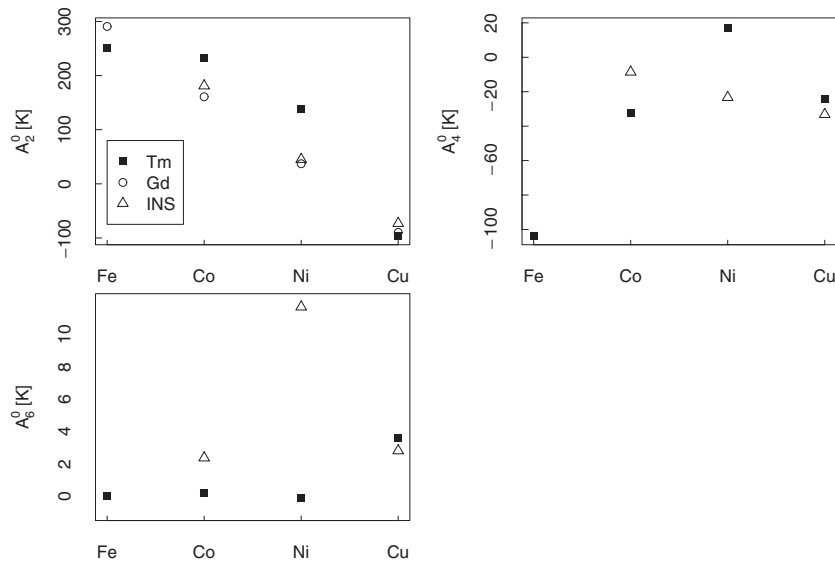


**Figure 7.** Variation of CF parameters obtained for  $TmT_2Si_2$  across the transition-metal series compared with the INS-derived parameters used to establish the ratios discussed in the text. The  $A_2^0$  CF parameter is compared with values derived from  $^{155}Gd$   $V_{zz}$  values [7, 8].

make the interpretation of the high-temperature spectra difficult. Nevertheless the fitted CF parameters are included in table 1.

Since  $\Delta E_Q$  is an unsigned energy splitting, it yields only the magnitude of  $V_{zz}$ . For  $T = Co$  and  $Ni$ , the fitted CF parameters correspond to a  $V_{zz}$  which is positive at low temperatures and crosses over to negative (the sign of the constant lattice contribution) at high temperatures. For  $T = Cu$ , the situation is reversed. There is no clear evidence for this crossover in any of the experimental  $\Delta E_Q$  data. In particular, the data for  $TmCo_2Si_2$  would appear to plateau out at 400 K without having dipped first to zero. The positive  $V_{zz}$  at low temperatures might also be considered to be inconsistent with the asymmetric nature of the  $^{169}Tm$  Mössbauer spectra observed for both  $TmCo_2Si_2$  and  $TmNi_2Si_2$ . If the line broadening is magnetic in origin (such as due to paramagnetic fluctuations) then the broader line might be expected to correspond to the  $m_I = \pm 1/2 \rightarrow \pm 3/2$  transition, implying a negative  $V_{zz}$  at low temperatures. However, from our experience, it is rarely the case in  $^{169}Tm$  Mössbauer spectroscopy that the negative-velocity absorption line is the broader. The  $TmFe_2Si_2$  spectra [10] are an exception. However, in that case, the line with the larger broadening switches from positive velocity to negative velocity as the temperature is increased, suggesting that other broadening mechanisms are involved.

#### 4. Discussion

A central thrust of this work has been to test CF parameters derived from INS data for  $ErCo_2Si_2$  (this work) and  $ErCu_2Si_2$  [4] against  $^{169}Tm$   $\Delta E_Q$  data for  $TmCo_2Si_2$  (this work) and  $TmCu_2Si_2$  [14]. One important outcome of this process is the improved CF interpretation for  $TmCu_2Si_2$ . Whereas the earlier CF analysis [14] was based on INS data for  $CeCu_2Si_2$ , the present CF parameters are in closer agreement with those reported for  $R = Ho$  and  $Er$ , that is for the heavy rare-earth neighbours of  $Tm$ . It was somewhat puzzling that the earlier CF analysis required a small  $A_2^0$  and a dominant  $A_4^0$ . However, this is no longer the case with

the new result. Instead a dominant negative  $A_2^0$  implies a  $c$ -axis magnetic alignment in the magnetic state (this is in reasonable agreement with the cosinusoidally modulated moment at  $30^\circ$  from the  $c$ -axis reported elsewhere [25]). These findings demonstrate the importance of a multiple-technique approach for unambiguous CF determination.

Trends in the CF parameters fitted to the  $^{169}\text{Tm}$   $\Delta E_Q$  data are shown in figure 7, where they are compared with the INS parameters that were used to arrive at the within-rank ratios  $r_4^4$  and  $r_6^4$ . Also included in this figure are the  $A_2^0$  parameters that were derived from the  $V_{zz}$  determined using  $^{155}\text{Gd}$  Mössbauer spectroscopy. In general,  $|A_6^0| < |A_4^0| < |A_2^0|$ . All three  $A_2^0$  values exhibit a steady decrease across  $T = \text{Fe, Co, Ni}$  and  $\text{Cu}$  and there is reasonable agreement between them. In fact, the outstanding agreement for the case of  $T = \text{Cu}$  implies that application of the ideal relationship between  $A_2^0$  and the lattice contribution to  $V_{zz}$  (as determined by  $^{155}\text{Gd}$  Mössbauer spectroscopy) may still be a useful device, despite Coehoorn's findings. There is less variation across the transition elements for  $A_4^0$  and  $A_6^0$ . The greatest discrepancy is observed for the  $A_4^0$  parameter determined for  $\text{TmFe}_2\text{Si}_2$  [10]. This is perhaps not unexpected given that experimental  $\Delta E_Q$  data were recorded only for  $T \leq 80$  K.

Some of the discrepancy between the CF interpretation of INS and  $^{169}\text{Tm}$   $\Delta E_Q$  data may lie in the nature of the experiments themselves. The INS and  $^{155}\text{Gd}$  Mössbauer measurements are both undertaken at liquid helium temperatures or slightly above, while the  $^{169}\text{Tm}$  measurements are recorded over a much wider temperature range. Temperature variation in the lattice parameters, and certainly any larger structural transitions (such as may occur for  $\text{TmNi}_2\text{Si}_2 \simeq 300$  K), will influence the local environment at the rare-earth site and, in turn, the values of the CF parameters. The possibility of a structural phase transition for  $\text{TmNi}_2\text{Si}_2$  will be looked at in further work.

## 5. Conclusions

The single rare-earth site in  $\text{ErCo}_2\text{Si}_2$  and  $\text{TmT}_2\text{Si}_2$  ( $T = \text{Co}$  and  $\text{Ni}$ ) has been probed using INS and  $^{166}\text{Er}$  Mössbauer spectroscopy ( $R = \text{Er}$ ) and  $^{169}\text{Tm}$  Mössbauer spectroscopy ( $R = \text{Tm}$ ). The saturation rare-earth moments for  $\text{ErCo}_2\text{Si}_2$  and  $\text{TmCo}_2\text{Si}_2$  were determined to be 7.8 and 6.5  $\mu_B$  respectively. New CF parameters were derived from the INS data for  $\text{ErCo}_2\text{Si}_2$ . These and other INS parameters from the literature have been tested against  $^{169}\text{Tm}$   $\Delta E_Q$  data and trends revealed. On the basis of this comparison, a more appropriate CF interpretation has been proposed for  $\text{TmCu}_2\text{Si}_2$ .

## Acknowledgment

This work was supported by a grant for source irradiation from the Australian Institute of Nuclear Science and Engineering.

## References

- [1] Szytuła A and Leciejewicz J 1989 *Handbook on the Physics and Chemistry of Rare Earths* vol 12, ed K A Gschneidner Jr and L Eyring (Amsterdam: Elsevier) ch 83, pp 133–208
- [2] Blanco J A, Garnier A, Gignoux D and Schmitt D 1998 *J. Alloys Compounds* **275–7** 565–568
- [3] Ivanov V and Szytuła A 1997 *J. Alloys Compounds* **262/263** 253–7
- [4] Goremychkin E A, Muzychka A Yu and Osborn R 1996 *JETP* **83** 738–46
- [5] Muzychka A Yu 1999 *Surf. Invest.* **14** 919–42
- [6] Nowik I, Felner I and Seh M 1980 *J. Magn. Magn. Mater.* **15–18** 1215–17
- [7] Dirken M W 1991 *PhD Thesis* Leiden
- [8] Coehoorn R, Buschow K H J, Dirken M W and Thiel R C 1990 *Phys. Rev. B* **42** 4645–55

- [9] Fåk B, Garnier A, Gignoux D, Kahn R and Schmitt D 1997 *Physica B* **233** 17–25
- [10] Umarji A M, Shenoy G K, Noakes D R and Dattagupta S 1984 *J. Appl. Phys.* **55** 2297–9
- [11] Blanco J A, Gignoux D, Gómez-Sal J C and Schmitt D 1992 *J. Magn. Magn. Mater.* **104–7** 1273–4
- [12] Blanco J A, Gignoux D and Schmitt D 1992 *Z. Phys. B* **89** 343–50
- [13] Gubbens P C M, de Vroege C F, Diviš M, Prokeš K, Mulder F M, Thiel R C and Buschow K H J 1995 *J. Magn. Magn. Mater.* **140–4** 909–10
- [14] Stewart G A and Zukrowski J 1982 *Crystalline Electric Field Effects in f-Electron Magnetism* ed R P Guertin (New York: Plenum) pp 319–25
- [15] Muzychka A Yu 1998 *JETP* **87** 162–74
- [16] Barandiaran J M, Gignoux D, Schmitt D, Gomez Sal J C and Rogriguez Fernandez J 1987 *J. Magn. Magn. Mater.* **69** 61–70
- [17] Gubbens P C M, van der Kraan A M and Buschow K H J 1989 *Phys. Rev. B* **39** 12 548–53
- [18] Leciejewicz J and Szytuła A 1983 *Solid State Commun.* **48** 55–6
- [19] Yakinthos J K, Routsis Ch and Schobinger-Papamantellos P 1983 *J. Magn. Magn. Mater.* **30** 355–8
- [20] Leciejewicz J, Kolenda M and Szytuła A 1983 *Solid State Commun.* **45** 145–8
- [21] Birgenau R J 1972 *J. Phys. Chem. Solids* **33** 59–68
- [22] Barnes R G, Mössbauer R L, Kankeleit E and Poindexter J M 1964 *Phys. Rev. A* **136** 175–89
- [23] Stewart G A 1985 *Hyperfine Interact.* **23** 1–16
- [24] Stewart G A and Gubbens P C M 1999 *J. Magn. Magn. Mater.* **206** 17–26
- [25] Allain Y, Bourée-Vigneron F, Oleś A and Szytuła A 1988 *J. Magn. Magn. Mater.* **75** 303–8